# Conformational Dynamics of a Y-Family DNA Polymerase during Substrate Binding and Catalysis As Revealed by Interdomain Förster Resonance Energy Transfer

Brian A. Maxwell,[†] Cuiling Xu,[‡] and Zucai Suo*,[†,‡]

[†]Ohio State Biophysics Program and [‡]Department of Chemistry and Biochemistry, The Ohio State University, Columbus, Ohio 43210, United States

S *Supporting Information*

ABSTRACT: Numerous kinetic, structural, and theoretical studies have established that DNA polymerases adjust their domain structures to enclose nucleotides in their active sites and then rearrange critical active site residues and substrates for catalysis, with the latter conformational change acting to kinetically limit the correct nucleotide incorporation rate. Additionally, structural studies have revealed a large conformational change between the apoprotein and the DNA−protein binary state for Y-family DNA polymerases. In previous studies [Xu, C., Maxwell, B. A., Brown, J. A., Zhang, L., and Suo, Z. (2009) *PLoS Biol. 7*, e1000225], a real-time Förster resonance energy transfer (FRET) method was developed to monitor the global conformational transitions of DNA polymerase IV from *Sulfolobus solfataricus* (Dpo4), a prototype Y-family enzyme, during nucleotide binding and incorporation by measuring changes in distance between locations on the enzyme and the DNA substrate. To elucidate further details of the conformational transitions of Dpo4 during substrate binding and catalysis, in this study, the real-time FRET technique was used to monitor changes in distance between various pairs of locations in the protein itself. In addition to providing new insight into the conformational changes as revealed in previous studies, the results here show that the previously described conformational change between the apo and DNA-bound states of Dpo4 occurs in a mechanistic step distinct from initial formation or dissociation of the binary complex of Dpo4 and DNA.
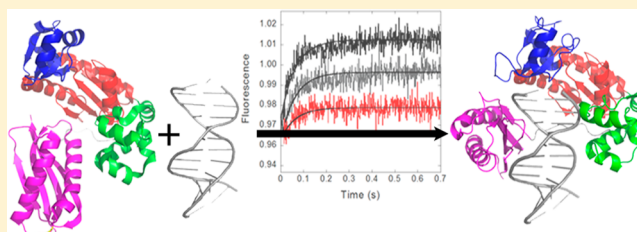
DNA polymerases are critical enzymes responsible for faithful replication of the genome. However, various DNA-damaging agents can lead to the formation of DNA lesions that often stall the progress of high-fidelity replicative DNA polymerases. The recently discovered Y-family DNA polymerases are able to bypass various types of DNA damage and rescue the stalled replication machinery in a process known as lesion bypass.[1] However, these Y-family lesion bypass polymerases are characterized by low fidelity, poor processivity, and a lack of intrinsic proofreading activity when replicating undamaged DNA.[2−7] Therefore, the switching between replicative and Y-family DNA polymerases during lesion bypass must be well regulated to prevent the introduction of unnecessary mutations by Y-family DNA polymerases. DNA polymerase IV from *Sulfolobus solfataricus* (Dpo4), the enzyme used in this study, is a model Y-family polymerase and has been extensively characterized through both structural[8−13] and kinetic studies.[7,14−17]

In solution, DNA polymerases, like many enzymes, are inherently flexible molecules that can undergo a variety of motions ranging from localized vibrations of side chains to translations and rotations of loops and secondary structures and even concerted global conformational transitions.[18] These conformational rearrangements are critical for the functions of enzymes, including catalysis,[19] signal transduction,[20]

allosteric regulation,[21] and structural-stability modification.[22] While substrate binding and catalysis usually occur at a specific "active site" in an enzyme involving only a few residues, structural changes are often observed at residues far from the active site and may involve rigid body motions of large protein domains or secondary structure elements consisting of many residues.

All DNA polymerases share a structurally conserved polymerase core with a "right hand" architecture, consisting of Finger, Thumb, and Palm domains, while Y-family DNA polymerases contain a unique Little Finger (LF) domain in addition to the polymerase core.[9,23−25] Upon binding to an incoming nucleotide, many DNA polymerases have been shown to undergo a Finger domain closing conformational change that helps bring functionally important enzyme residues in contact with the nucleotide and serve as a fidelity check point for preventing misincorporations.[26] Crystal structures of Y-family DNA polymerases such as Dpo4 bound to DNA do not reveal a large domain swing upon nucleotide binding analogous to the Finger domain closing observed for other DNA polymerases.[9,11] Nevertheless, stopped-flow studies monitoring

both Trp fluorescence[27] and FRET[28] as well as hydrogen–deuterium exchange experiments[29] have provided information about global conformational changes that occur throughout each of the four domains of Dpo4 during correct nucleotide binding and catalysis. Furthermore, it was shown that these conformational changes are altered by the presence of a lesion in the DNA template.[30,31] Additionally, X-ray crystallography and tryptophan fluorescence studies have shown that Dpo4 undergoes a large conformational change from the apo form to the DNA-bound binary state characterized by a rotation of the LF domain relative to the polymerase core.[8] In a recent study, this conformational change was proposed to be involved in polymerase switching during lesion bypass.[32]

Our previous studies made use of two FRET systems to monitor changes in distance either between the DNA substrate and each domain of Dpo4 or between the Finger and LF domain.[28] Here, we have further investigated the conformational changes during nucleotide binding and incorporation by utilizing a FRET system with a donor in the LF domain and an acceptor in the Palm domain as well as an additional FRET system with a donor in the Palm domain and an acceptor in each of the remaining domains of Dpo4. Furthermore, both intrinsic tryptophan fluorescence and FRET spectroscopy were used to investigate the conformational changes of the LF domain relative to the polymerase core of Dpo4 during DNA binding and dissociation.

■ MATERIALS AND METHODS

Materials. The cysteine reactive dye, 7-(diethylamino)-3-(4′-maleimidylphenyl)-4-methylcoumarin (CPM), was obtained from Invitrogen. The DNA substrate consisted of two synthetic oligodeoxynucleotides synthesized by Integrated DNA Technologies (IDT), a 21-mer primer (5′-CG AGC CGT CGC ATC CTA CCG C-3′) and a 30-mer template (5′-G ATG CTG CAG CGG TAG GAT GCG ACG GCT CG-3′). The primer 21-mer in the DNA substrate 21/30-mer is either normal (DNA^{OH}) or 3′-dideoxy-terminated (DNA^H) as synthesized by Integrated DNA Technologies. The DNA substrates were purified by denaturing polyacrylamide gel electrophoresis (17% polyacrylamide and 8 M urea), and the concentrations were determined by UV absorbance at 260 nm using the corresponding extinction coefficients.

Mutagenesis, Purification, and Labeling of Dpo4. The expression plasmid containing the *S. solfataricus dpo4* gene was constructed as described previously.[14] Mutations were introduced by using the Quikchange kit (Stratagene) according to the manufacturer's instructions. First, to avoid the ambiguity of labeling, the sole native cysteine of Dpo4 was mutated to serine (C31S). Second, using the C31S mutant as a template, a unique intrinsic fluorescence donor Trp residue was introduced individually into the LF (Y274W) or Palm (Y108W) domain of Dpo4. Finally, on the basis of this double mutant, a single cysteine was individually substituted on the domains of Dpo4 to serve as the specific site of attachment for the acceptor CPM. These mutations were confirmed by DNA sequencing and are shown in Figure 1. The Dpo4 mutants were expressed and purified as described for wild-type (wt) Dpo4.[14] The concentration of each mutant was determined spectrophotometrically at 280 nm using a molar extinction coefficient of 28068 M^{-1} cm^{-1}, which was calculated on the basis of the sequence of wt Dpo4 containing a single Tyr to Trp mutation.

The labeling of Dpo4 mutants was performed in the labeling buffer [50 mM Tris-HCl (pH 7.5), 0.15 M NaCl, 10% glycerol,
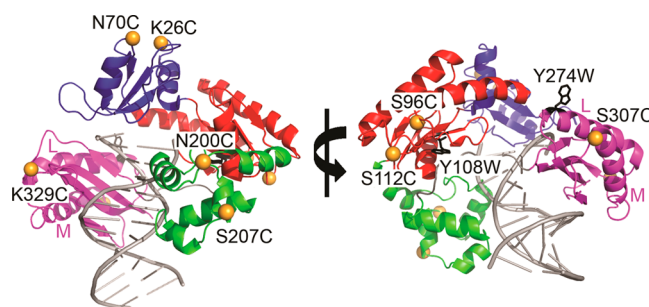

Figure 1. Locations for the introduction of a fluorophore into the binary structure of Dpo4 and DNA. The positions for attachment of a CPM acceptor fluorophore are shown as orange spheres, and the Trp donor residues are shown as a black ball and stick model. The Finger, Thumb, Palm, and LF domains are colored blue, green, red, and purple, respectively, with α helices L and M in the LF domain indicated. The DNA substrate is colored gray.

and 0.5 mM TCEP]. A 10–20-fold molar excess of CPM was added dropwise to a 50–100 μM protein solution. The labeling reaction was allowed to proceed while the mixture was slowly and constantly mixed at 4 °C overnight, and unreacted dye was quenched by adding an equimolar amount of glutathione. Labeled protein was separated from the unbound fraction of dye by size exclusion gel filtration (Sephadex G-25 resin). Eluted protein was extensively dialyzed against the Dpo4 storage buffer and stored as aliquots at −80 °C. The protein concentration was determined by using the Bradford assay (Bio-Rad) with wt Dpo4 as a standard, and the degree of labeling was typically ≥90%.

Buffers. All experiments, if not specified, were conducted in buffer R, consisting of 50 mM HEPES (pH 7.5) at 20 °C, 6 mM MgCl$_2$, 50 mM NaCl, 0.1 mM EDTA, 1 mM DTT, and 10% glycerol.

Steady-State Fluorescence Spectroscopy Assays. Steady-state fluorescence spectra were recorded on a Fluoromax-4 instrument (Jobin Yvon Horiba). The assay solution typically contained 200 nM CPM-labeled mutant proteins in the reaction buffer equilibrated at 20 °C. To this solution were added sequentially 300 nM DNA substrate and 1 mM dNTP. Fluorescence spectra were recorded after each addition of DNA and dNTP at the excitation wavelength of tryptophan (290 nm) with slits set at 5 nm for both excitation and emission. Reported spectra were corrected for dilution and for the intrinsic fluorescence of buffer components and dTTP, which were measured in the absence of DNA and any protein.

Circular Dichroism Spectroscopy Assays. Circular dichroism (CD) spectra were recorded using a model 62A DS spectrometer (Aviv) in a 1 mm path length cuvette at 37 °C. The spectra were recorded in the buffer [25 mM sodium phosphate (pH 7.5), 50 mM NaCl, and 5 mM MgCl$_2$]. Data points from 270 to 200 nm were recorded for Dpo4 and its mutants at 1 nm intervals. Each data point was averaged for 5 s. All measurements were corrected for the background signal.

Stopped-Flow Assays. Stopped-flow fluorescence experiments were performed on an Applied Photophysics SX20 system at a constant temperature of 20 °C. Samples were excited at 290 nm, and the fluorescence of Trp or CPM was monitored by using a 305 or 420 nm cutoff filter, respectively. Again, the slits were set at 5 nm for both excitation and emission. All reported concentrations represent the final concentrations of components after mixing. The rate for each

fluorescent phase was determined by fitting a stopped-flow fluorescence trace using the KinTek Explorer global fitting software.[33] The software was set to fit each trace using a single- or double-exponential equation depending on the number of observed FRET phases. Reported rates and the associated errors are reported as averages and standard deviations determined from fits to traces acquired in multiple repeat stopped-flow mixing experiments.

■ RESULTS

Construction of an Interdomain FRET System. To monitor changes in distance between two domains, Dpo4 mutants containing a single-tryptophan FRET donor fluorophore and a single Cys for labeling with the acceptor fluorophore CPM were generated (Figure 1 and Table 1).

Table 1. Distances[a] between the Trp Donor and Residues with an Attached CPM Acceptor Estimated from Crystal Structures

Distances between Y274W on the LF Domain and Residues on the Individual Domains of Dpo4				
	distance (Å)			
	Palm		Thumb	
protein form	S112C	S96C	N200C	S207C
apo[b]	28.4	28.4	20.2	22.8
binary[c]	38.1	31.0	44.7	49.5
ternary[d]	38.6	31.3	45.8	51.8

Distances between Y108W on the Palm Domain and Residues on the Individual Domains of Dpo4					
	distance (Å)				
	LF		Finger		Thumb
protein form	K329C	S307C	N70C	K26C	N200C	S207C
apo[b]	44.7	28.8	38.4	32.7	29.4	31.9
binary[c]	42.6	35.2	38.3	31.6	28.4	32.5
ternary[d]	42.6	35.4	38.2	31.7	28.5	32.5

[a]Estimated distances do not account for the flexible carbon linker used to attach the CPM fluorophore to the introduced Cys residues. [b]Calculated distance between the C_α atom of Dpo4 residues in the apo structure of Dpo4 (PDB entry 2RDI). [c]Calculated distance between the C_α atom of Dpo4 residues based on the crystal structure of the Dpo4·DNA binary complex (PDB entry 2RDJ). [d]Calculated distance between the C_α atom of Dpo4 residues based on the crystal structure of the Dpo4·dideoxy-DNA·matched dATP ternary complex (PDB entry 2AGQ).

Because wt Dpo4 contains no native Trp residues, single Trp residues were introduced separately into the Palm (Y108W) or LF (Y274W) domain via site-directed mutagenesis. To avoid ambiguity in CPM labeling, the single native Cys (C31) of Dpo4 was mutated to Ser. Using the expression DNA plasmid encoding a Dpo4 mutant containing a single Trp and no Cys, single Cys residues were introduced into various positions throughout Dpo4 for labeling with CPM (Figure 1 and Materials and Methods). For the sake of simplicity, triple Dpo4 mutants in this study will be cited by the single Trp mutation and the introduced Cys only, e.g., Y274W-S96C. Enzymatic activities of CPM-labeled, e.g., Y274W-S96C[CPM], and unlabeled Dpo4 mutants, e.g., Y274W-S96C, were measured under single-turnover conditions using ^{32}P-based kinetic assays (Materials and Methods). The observed rates of nucleotide incorporation (k_{obs}) for the unlabeled and CPM-labeled Dpo4 mutants were

similar to that measured for the wt enzyme (Table 2), indicating that neither the mutations nor the labeling had a

Table 2. Observed Rates (k_{obs}) of Incorporation of dTTP into DNA[OH] Catalyzed by Dpo4 or Each of Its CPM-Labeled Mutants at 20 °C under Single-Turnover Reaction Conditions

enzyme	$k_{obs}{}^{a}$ (s^{-1})
wt Dpo4	0.8 ± 0.1
Y274W-S96C[CPM]	0.8 ± 0.1
Y274W-S112C[CPM]	0.54 ± 0.04
Y108W-N70C[CPM]	0.33 ± 0.03
Y108W-K26C[CPM]	0.39 ± 0.03
Y108W-K329C[CPM]	0.47 ± 0.04
Y108W-S307C[CPM]	0.35 ± 0.03
Y108W-S207C[CPM]	0.39 ± 0.03
Y108W-N200C[CPM]	0.36 ± 0.02

[a]Obtained from single-turnover kinetic assays in which a preincubated solution of a Dpo4 mutant (180 nM) and 5′-^{32}P-labeled DNA[OH] (30 nM) was rapidly mixed with dTTP (1 mM) and subsequently quenched at various time intervals with 0.37 M EDTA and the plot of product concentration vs time was fit to the single-exponential equation [product] = $A[1 - \exp(-k_{obs}t)]$ to yield an observed rate k_{obs} and a reaction amplitude (A).

significant effect on the polymerase activity of Dpo4. Furthermore, the circular dichroism spectra of the unlabeled mutants confirmed that the mutations did not alter the secondary structure of Dpo4 (Figure S1 of the Supporting Information).

Steady-State Fluorescence of Dpo4 Mutants Y108W and Y274W. To gain insight into the local environment of the engineered Trp residues, fluorescence emission spectra for unlabeled Dpo4 mutants Y108W and Y274W were recorded (Figure 2A). The emission maximum for Y108W was approximately 320 nm, characteristic of a buried Trp residue, while the red-shifted emission maximum (354 nm) of Y274W is consistent with a higher degree of solvent exposure.[8,34] When a normal DNA substrate 21/30-mer was bound [DNA[OH] (Materials and Methods)], a significant reduction in Trp fluorescence was observed for both Y108W (30.3%) and Y274W (21.6%). Following DNA binding, dTTP incorporation into the E·DNA complex resulted in a further decrease in Trp fluorescence. As both DNA and dTTP absorb at 290 nm, the observed decreases in Trp fluorescence upon their additions may be primarily due to inner filter effects resulting from their absorbance of the excitation light.[35] However, the difference in fluorescence attenuation for the two mutants upon the addition of DNA (30.3 and 21.6% for Y108W and Y274W, respectively) suggests that protein conformational changes or interaction with the DNA substrate could also contribute to the changes in Trp fluorescence, as inner filter effects would be expected to decrease the Trp fluorescence of the two mutants to the same extent.

Steady-state fluorescence spectra of mutants Y274W-S96C[CPM] and Y108W-K329C[CPM] (panels B and C of Figure 2, respectively, black traces) show that the attachment of CPM to a unique cysteine residue had a significant quenching effect on the Trp fluorescence of both Y274W and Y108W, upon excitation at 290 nm, the peak excitation wavelength of Trp. Concomitantly, an intense acceptor peak centered at 472 nm was observed, which was a strong indicator of the efficient
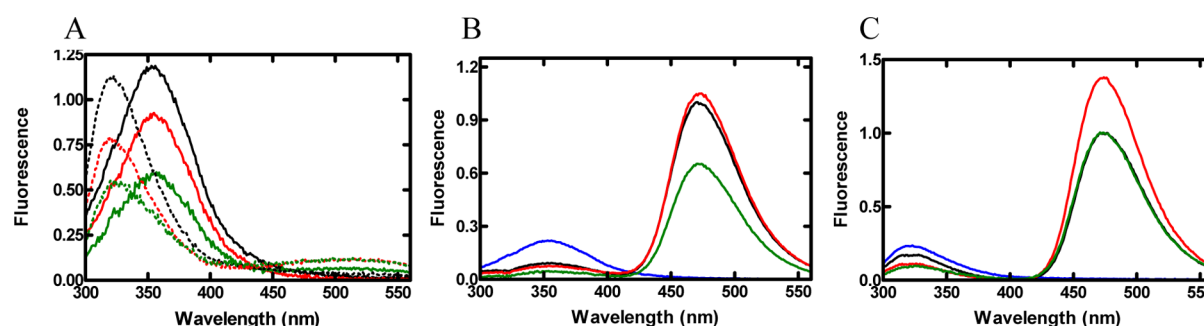
Figure 2. Steady-state fluorescence spectra of Dpo4 mutants. The emission spectra of Dpo4 mutants (200 nM) were recorded at 20 °C with an excitation wavelength of 290 nm. (A) Emission spectra of mutants Y108W-N70C (dotted) and Y274W-N70C (solid) with either the mutants alone (black) or after sequential additions of 300 nM DNA^{OH} (red) and 1 mM dTTP (green). (B and C) Emission spectra of CPM-labeled mutants Y274W-N70C^{CPM} and Y108W-K329C^{CPM}, respectively, with either the mutants alone (black) or after sequential additions of 300 nM DNA^{OH} (red) and 1 mM dTTP (green). The emission spectra for the mutants prior to labeling with CPM are colored blue.
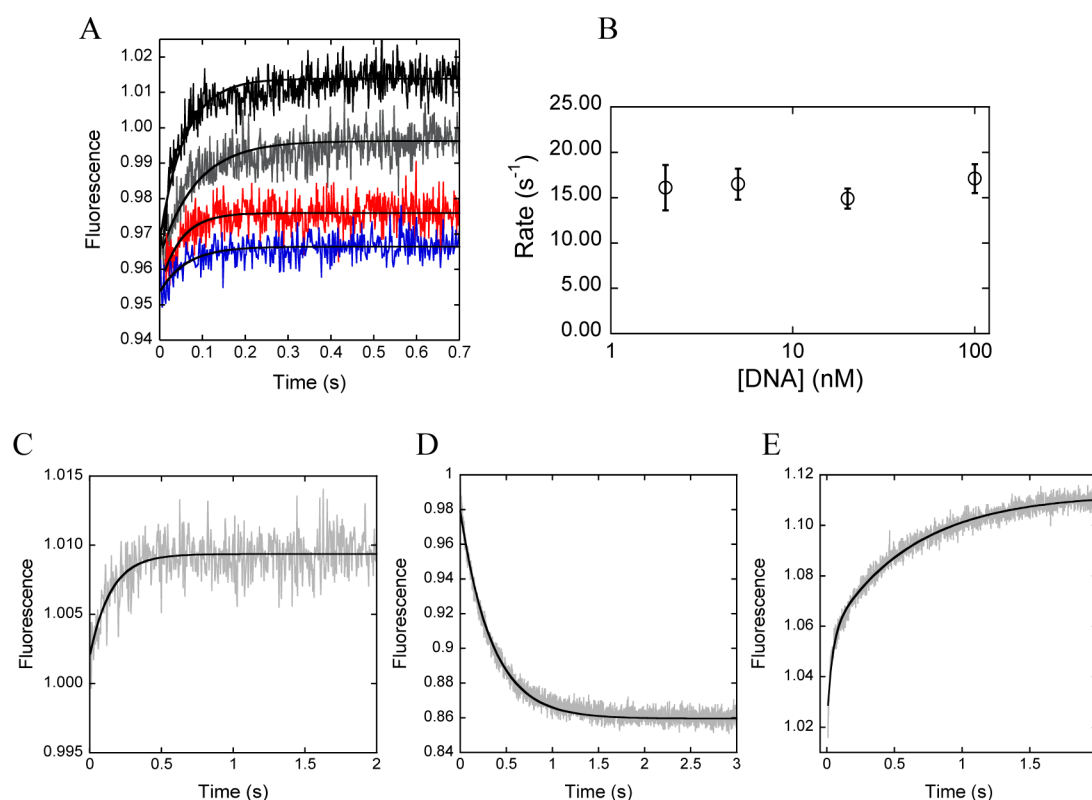

Figure 3. Conformational changes upon DNA binding. (A) Dpo4 mutant Y108W-K329C^{CPM} (100 nM) was rapidly mixed with 2 nM (blue), 5 nM (red), 20 nM (gray), or 100 nM (black) DNA^{OH}, and the CPM fluorescence was measured upon excitation of Trp at 290 nm. Data from each trace were fit to a single-exponential equation, $A[1 - \exp(kt)]$ (A, black lines), and the observed rates (k) were plotted vs DNA concentration (B). Trp fluorescence of mutant Y108W (C) or the CPM fluorescence of mutant Y108W-K329C^{CPM} (D) upon mixing of a solution of 100 nM Dpo4 mutant and 100 nM DNA^{OH} with 2 μM unlabeled wt Dpo4. (E) CPM fluorescence upon mixing of a preincubated solution of 100 nM wt Dpo4 and 100 nM DNA^{OH} with 2 μM Y108W-K329C^{CPM}.

transfer of energy from Trp to CPM. The addition of the substrate DNA^{OH} resulted in a very slight increase in the acceptor CPM fluorescence for mutant Y274W-K96C^{CPM} and a dramatic increase for mutant Y108W-K329C^{CPM} (~30%) (Figure 2B,C, green traces). These results suggest that the Y108W-K329C^{CPM} FRET pair is better suited for dynamically investigating the conformational change in the LF domain relative to the polymerase core. Addition of dTTP to the binary complexes of the Dpo4 mutants with DNA^{OH} resulted in a dramatic decrease in CPM fluorescence for both Y274W-S96C^{CPM} (38%) and Y108W-K329C^{CPM} (28%), which is predominantly due to inner filter effects from the absorbance

of the excitation light by dTTP with a high concentration (1 mM), rather than resulting only from a change in FRET efficiency as both CPM and Trp fluorescence intensities were reduced (Figure 2B,C). However, as described above, the differences observed for the two mutants in panels B and C of Figure 2 suggest that conformational changes may also contribute to the changes in fluorescence. All other Dpo4 mutants listed in Table 2 exhibited similar trends consistent with the distance variation based upon the crystal structure analysis of apo and binary complexes (data not shown).

Conformational Change upon Binding of Dpo4 to DNA. To further investigate the observed conformational

change in the LF domain relative to the polymerase core during DNA binding, rapid mixing experiments were performed using the Y108W or Y108W-K329C^{CPM} mutant in a stopped-flow apparatus upon excitation of Trp at 290 nm. Notably, all stopped-flow experiments in this study were performed at 20 °C to be consistent with published stopped-flow FRET studies with Dpo4 that showed that some FRET changes are not easily observed at higher temperatures.[28,30] Mixing of Dpo4 mutant Y108W with DNA in the absence of the CPM acceptor did not result in a detectable time-dependent change in fluorescence (Figure S2A of the Supporting Information), indicating that the quenching of Trp fluorescence observed in the steady-state assay (Figure 2A) occurred within the dead time (∼1 ms) of the stopped-flow apparatus, as would be expected for quenching due to inner filter effects. However, mixing of Y108W-K329C^{CPM} with DNA resulted in a measurable rapid increase in CPM fluorescence (Figure 3A), consistent with steady-state FRET measurements (Figure 2C). Interestingly, the rate of this fluorescence change (∼16 s^{-1}) did not increase as the concentration of DNA was increased from 2 to 100 nM while the enzyme concentration was held constant at 100 nM (Figure 3B). Notably, at concentrations of <2 nM, the amplitude of the fluorescence change was too low to be easily detected in the stopped-flow apparatus. The observation of a constant rate over a nearly 2 order of magnitude increase in DNA concentration suggests that the change in fluorescence may correspond to a conformational change that occurs at a step distinct from the formation of the Dpo4·DNA binary complex as the later step is expected to be a second-order process with an observed rate that increases linearly with DNA concentration. Several assays were also performed to investigate the reverse conformational change upon dissociation of the Dpo4·DNA complex. The mixing of a preincubated solution of the Y108W mutant and DNA with a 20-fold excess of tryptophan-free wt Dpo4 to sequester any DNA that dissociates from the labeled enzyme resulted in a time-dependent increase in Trp fluorescence (Figure 3C). This result is consistent with the steady-state spectra that show that the fluorescence of Y108W was decreased by 30.3% upon addition of DNA (Figure 2A). Moreover, the decrease is ∼10% more with the Y108W mutant than with the Y274W mutant, suggesting that a conformational change upon DNA binding is partially responsible for the observed decrease in Trp fluorescence (Figure 2A). When the experiment was performed by mixing the preincubated, labeled Y108W-K329C^{CPM}·DNA complex with excess unlabeled wt Dpo4, a large decrease in CPM fluorescence was observed (Figure 3D). Notably, the rate of the CPM fluorescence change for the labeled Y108W-K329C^{CPM} (3.3 ± 0.2 s^{-1}) was <2-fold slower than the observed rate for the Y108W mutant (6 ± 1 s^{-1}) (Figure 3C,D). The latter rate may be less accurate because of the low signal-to-noise ratio (Figure 3C). Using an alternative approach, a preincubated solution of unlabeled Dpo4 and DNA was mixed with an excess of the labeled Y108W-K329C^{CPM} mutant, which resulted in a biphasic increase in CPM fluorescence (Figure 3E). The faster phase rate (15.1 ± 0.6 s^{-1}) was similar to the rate measured for the forward conformational change rate (Figure 3B) and likely results from an initial binding of the small fraction of DNA that was not bound to the unlabeled Dpo4 during the preincubation prior to mixing. The slower phase likely results from the binding of DNA to the labeled Dpo4 after it has dissociated from unlabeled Dpo4 with the observed rate (1.7 ± 0.2 s^{-1}), which is a function of the rates of both the forward (∼16 s^{-1})

and reverse (3.3 s^{-1}) conformational changes. Together, these results suggest that Dpo4 utilizes a DNA binding mechanism with a conformational change occurring at a step different from the formation and dissociation of the Dpo4·DNA binary complex.

Conformational Dynamics during Correct Nucleotide Incorporation. To characterize the dynamics of conformational transitions employed by Dpo4 during correct nucleotide insertion, a solution containing a CPM-labeled Dpo4 mutant preincubated with DNA^{OH} was rapidly mixed with the correct dTTP, and the CPM fluorescence was monitored upon excitation at 290 nm. Only the acceptor CPM fluorescence was monitored, as the Trp fluorescence was too weak to be accurately measured in the presence of the CPM acceptor. Notably, no time-dependent change in fluorescence was observed upon mixing of dTTP with labeled Dpo4 in the absence of the DNA (Figure S2B of the Supporting Information), suggesting that the fluorescence changes resulting from inner filter effects observed in the steady-state experiments (Figure 2) occurred within the mixing dead time (∼1 ms) of the stopped-flow instrument. Additionally, no change in Trp fluorescence was observed in control experiments in the absence of the CPM acceptor (Figure S2C of the Supporting Information), indicating that any observed changes in CPM fluorescence would be primarily due to changes in FRET efficiency rather than changes in the local environment of the Trp probe.

In a previously published study, the conformational changes of the Finger domain (N70C and K26C) relative to the LF domain (Y274W) were investigated through two labeled mutants, Y274W-N70C^{CPM} and Y274W-K26C^{CPM}.[28] Here, similar assays were performed to investigate the conformational changes of the Palm domain at the residues of S96C and S112C relative to the LF domain. The distances between potential labeling residues in the Thumb domain, e.g., S207C and N200C, and the Y274W residue in the LF domain in the binary and ternary structures are greater than $R_0 ± 0.5R_0$, where R_0 is the Förster distance of 30 Å for a Trp−CPM FRET pair (Table 1). Therefore, changes in distances between these two domains during nucleotide binding and incorporation could not be accurately measured using this FRET system. When a preincubated solution of the labeled mutant Y274W-S112C^{CPM} and DNA was mixed with the correct dTTP, a biphasic fluorescence change was observed, consisting of a rapid [17 s^{-1} (Table 3)] decrease phase (P$_1$) followed by a slow [0.3 s^{-1} (Table 3)] fluorescence increase phase (P$_2$) (Figure 4A, black trace). Notably, similar results were observed previously for the motion of the Finger domain relative to the LF domain.[28] The signal-to-noise ratio for the Y274W-S96C^{CPM} mutant was significantly lower than for the Y274W-S112C^{CPM} mutant, and consequently, a second P$_2$ phase could not be clearly distinguished (Figure 4B), indicating that this FRET pair was not as well suited for measuring conformational changes. These results, along with those from previous studies,[28] indicate that the LF domain moved away from both the Finger and Palm domains and then closed back in toward the polymerase core to complete one catalytic cycle.

Next, the conformational transitions of the LF, Finger, and Thumb domains relative to the Trp donor (Y108W) in the Palm domain were investigated. The fluorescence changes observed for this system were much more varied than those obtained with the Trp donor (Y274W) located in the LF domain. Finger domain residue N70C (Figure 5A and Table 3)

Table 3. Rates of Stopped-Flow Fluorescence Changes at 20 °C

domain	CPM-labeled residue	phase	rate (s⁻¹) with DNA^{OH}	with DNA^{H}
		Relative to the Trp Donor (Y274W) in the LF Domain		
Palm	S112C	P$_1$	17 ± 4	19 ± 1
		P$_2$	0.3 ± 0.1	–
	S96C	P$_1$	11.4 ± 1.7	12.2 ± 1.5
		P$_2$	–	–
		Relative to the Trp Donor (Y108W) in the Palm Domain		
Finger	N70C	P$_1$	23 ± 6	20 ± 4
		P$_2$	0.57 ± 0.2	–
	K26C	P$_1$	5.2 ± 0.6	3.7 ± 0.6
		P$_2$	–	–
LF	K329C	P$_1$	18 ± 4	17 ± 2
		P$_2$	0.42 ± 0.07	–
	S307C	P$_1$	20 ± 4	20 ± 5
		P$_2$	0.27 ± 0.07	0.27 ± 0.06
Thumb	N200C	P$_1$	17 ± 4	17 ± 3
		P$_2$	–	–
	S207C	P$_1$	16 ± 7	17 ± 5
		P$_2$	0.16 ± 0.03	–

showed a biphasic trace similar to that observed for the same residue relative to the LF domain in published studies.[28] Notably, the amplitude of the fluorescence change for the Finger mutant Y108W-K26C^{CPM} was significantly lower than that observed for the other site (N70C) on the Finger domain, and the P$_2$ phase was less obvious (Figure 5B). The Thumb domain mutant Y108W-S207C^{CPM} produced changes in fluorescence in the opposite direction versus those of the Finger domain mutants, with a rapid increase phase (P$_1$) and a second, slow decrease phase (P$_2$) (Figure 5C). In contrast, the other Thumb domain mutant, Y108W-N200C^{CPM}, displayed only a fast fluorescence decrease phase (P$_1$) while a P$_2$ phase could not be distinguished. Surprisingly, relative to Y108W in the Palm domain, the two LF domain residues (S307C and K329C) also appeared to move in opposite directions (Figure 5E,F). As with residue S207C, residue K329C yielded a rapid increase P$_1$ phase followed by a slow decrease P$_2$ phase (Figure 5E). In contrast, residue S307C displayed a rapid decrease P$_1$ phase followed by a slow increase P$_2$ phase (Figure 5F), which was consistent with the result obtained with Trp in the LF

domain (Y274W) and the labeled Cys residue in the Palm domain (S112C) (Figure 4A). Thus, LF residues S307C and Y274W appear to move in the opposite direction compared to the other LF residue, K329C, relative to the Palm domain. Notably, the rates of each phase were similar for all mutants except K26C (Table 3).

Conformational Dynamics during Correct dNTP Binding with a Dideoxy-Terminated DNA Substrate. To explore the origins of the observed biphasic kinetics, a nonextendible substrate 21/30-mer DNA^{H} (Materials and Methods) was employed to distinguish between events occurring before and after phosphodiester bond formation. When nucleotide incorporation was prevented, the P$_2$ phase for all but one of the mutants was not observed upon mixing with dTTP while the rapid P$_1$ phase remained unchanged at an average rate of approximately 20 s⁻¹ (Table 3 and Figures 4 and 5). This suggests that, for these mutants, P$_1$ represents a precatalytic conformational change while P$_2$ corresponds to a transition taking place after nucleotide incorporation. Additionally, the rate of P$_2$ is similar to the rate for the rate-limiting step in nucleotide incorporation under single-turnover conditions for each mutant [average k_{obs} of 0.5 s⁻¹ (Table 2)]. The one exception was mutant Y108W-S307C^{CPM} (Figure 5F), for which the P$_2$ phase was essentially identical for both DNA^{OH} and DNA^{H} substrates. These results indicate that Dpo4 may undergo an additional transition after the initial fast conformational change that is independent of phosphodiester bond formation. However, this conclusion needs to be verified by further studies.

■ DISCUSSION

The FRET-based methodology is a very instructive approach for investigating enzyme dynamics. It not only allows for identification and rate determination of conformational changes but also can provide insights into the directional and rotational nature of those motions. Despite the fact that X-ray crystallography has not revealed large conformational shifts in Dpo4 upon nucleotide binding or incorporation, previous FRET studies have characterized pre- and postcatalytic conformational changes in all four domains of Dpo4 by monitoring the changes in distance between the protein and the DNA substrate.[28,30] The results of this investigation uncovered additional details of these conformational changes as well as conformational changes involved in DNA binding by
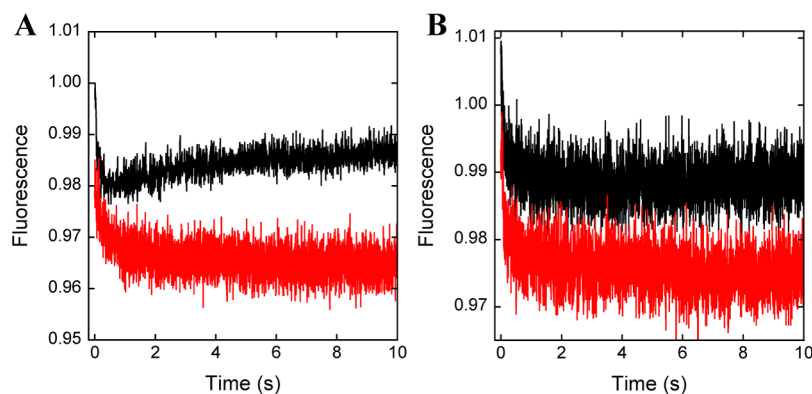

Figure 4. Conformational motion of the Palm domain relative to the LF domain during nucleotide binding and incorporation. Changes in CPM fluorescence upon excitation of Trp at 290 nm are shown after mixing of 1 mM dTTP with a preincubated solution of a Dpo4 mutant (200 nM) and either DNA^{OH} (300 nM, black) or DNA^{H} (300 nM, red) at 20 °C: (A) Y274W-S112C^{CPM} and (B) Y274W-S96C^{CPM}.
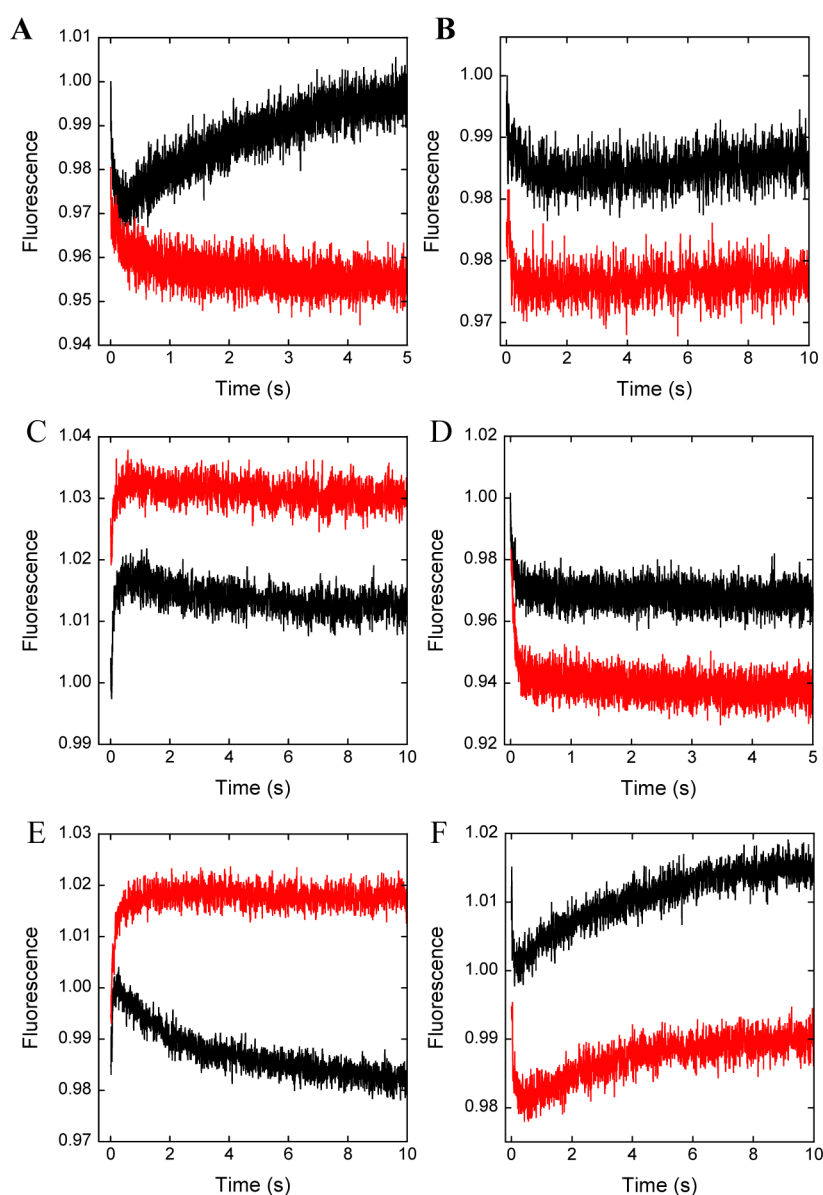
Figure 5. Conformational motions of the Finger, Thumb, and LF domains relative to the Palm domain during nucleotide binding and incorporation. Changes in CPM fluorescence upon excitation of Trp at 290 nm are shown after mixing of 1 mM dTTP with a preincubated solution of a Dpo4 mutant (200 nM) and either DNA^{OH} (300 nM, black) or DNA^H (300 nM, red) at 20 °C: (A) Y108W-N70C^{CPM}, (B) Y108W-K26C^{CPM}, (C) Y108W-S207C^{CPM}, (D) Y108W-N200C^{CPM}, (E) Y108W-K329C, and (F) Y108W-S307C^{CPM}.

monitoring changes in distance between pairs of locations on the protein itself.

Published crystallographic studies revealed that Dpo4 undergoes a significant conformational change from the apo state to the DNA-bound state with a 131° rotation of the LF domain relative to the polymerase core.[8] The results here show that this conformational change in the LF domain occurs at a rate of ~16 s^{-1} and is independent of DNA concentration over nearly 2 orders of magnitude (Figure 3A,B). In contrast, in a previous study that monitored FRET between labeled DNA and a labeled DNA polymerases to directly monitor formation of the E·DNA binary complex, the observed rate of change in fluorescence upon mixing of the polymerase with the DNA was found to increase linearly with an increasing protein concentration,[36] as would be expected for a second-order binding process. Thus, the results of this study are consistent with a multistep binding mode in which this conformational

change occurs in a step distinct from formation of the Dpo4· DNA complex. Two potential models for the binding of Dpo4 to DNA are possible: either the conformational change occurs after the initial binding of Dpo4 to DNA (Figure 6A), or Dpo4 is in equilibrium between two conformations, only one of which is capable of binding to DNA (Figure 6B). The crystal structure of apo Dpo4 shows that the LF domain actually occupies the DNA binding cleft of the polymerase core,[8] which would support the model shown in Figure 6B, as the LF domain would need to change its conformation to allow DNA to bind to Dpo4.

Previous kinetic studies[7] have indicated that the rate-limiting step in steady-state catalysis is the slow dissociation of the DNA from Dpo4 (0.02 s^{-1} at 37 °C), several orders of magnitude lower than the rates of the conformational change measured here at 20 °C by Trp fluorescence [6 s^{-1} (Figure 3C)] or by FRET monitoring of CPM fluorescence [3.3 s^{-1} (Figure 3D)].

A

$$E^{apo} + DNA \rightleftharpoons E^{apo} \bullet DNA \rightleftharpoons E \bullet DNA$$

B

$$E^{apo} \rightleftharpoons E + DNA \rightleftharpoons E \bullet DNA$$

C

Step 1   Step 2   Step 3   Step 4   Step 5   Step 6

$$E^{apo} \underset{k_{-1}=3.3\,s^{-1}}{\overset{k_1=16\,s^{-1}}{\rightleftharpoons}} E + DNA \underset{k_{-2}\,fast}{\overset{k_2}{\rightleftharpoons}} E\bullet DNA^* \underset{k_{-3}\le0.02\,s^{-1}}{\overset{k_3}{\rightleftharpoons}} E\bullet DNA \overset{dNTP}{\rightleftharpoons} E\bullet DNA_n\bullet dNTP \overset{P_1}{\rightleftharpoons} E'\bullet DNA_n\bullet dNTP \rightleftharpoons E''\bullet DNA_n\bullet dNTP$$

Step 7

$$E\bullet DNA^*_{n+1} \overset{PP_i}{\rightleftharpoons} E\bullet DNA^*_{n+1}\bullet PP_i \rightleftharpoons E'\bullet DNA^*_{n+1}\bullet PP_i \rightleftharpoons E''\bullet DNA^*_{n+1}\bullet PP_i$$

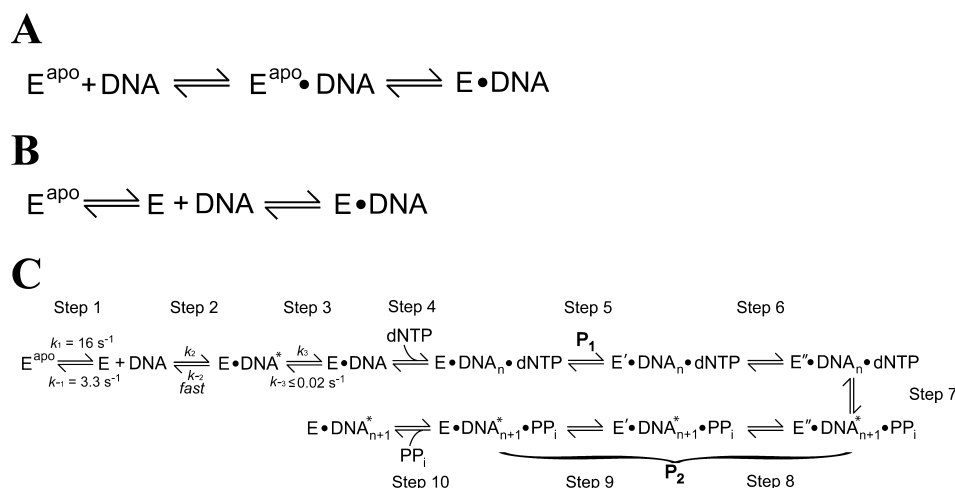Step 10   Step 9 P_2 Step 8

Figure 6. Possible models for the mechanism of binding of Dpo4 to DNA and subsequent nucleotide incorporation. Two alternative DNA binding models are shown (A and B) along with a full catalytic mechanism (C). E·DNA* and E·DNA represent nonproductive and productive binary complexes, respectively. E^{apo}, E, E′, and E″ represent four different conformations of Dpo4. PP_i denotes pyrophosphate. P_1 and P_2 are the two fluorescent phases observed in Figures 4 and 5.

In the ^{32}P-based kinetic assay, the loss of product formation was measured upon mixing with dNTP for a fixed time interval after a preincubated solution of Dpo4 and radiolabeled DNA had been mixed with an excess of unlabeled trap DNA for varying time intervals.[7] This difference in rates obtained from the two techniques lends further support to a model in which the conformational change and DNA binding represent distinct steps. Notably, from these results, the possibility of a more complex binding process with additional steps in which Dpo4 adopts conformations intermediate between those observed in the apo and DNA-bound crystal structures cannot be ruled out.

To account for the results from fluorescence assays in this study, along with those from previous kinetic and structural studies, an expanded three-step model for DNA binding has been added to the previously proposed catalytic mechanism of Dpo4 (Figure 6C).[28] In this model, it is proposed that, in the absence of DNA, the LF domain of Dpo4 is in equilibrium between two conformations (step 1, Figure 6C), only one of which (E) allows for DNA binding, and that after an initial rapid binding to DNA (step 2, Figure 6C), the binary complex is also in equilibrium between a nonproductive state and a productive state (step 3, Figure 6C), only one of which (E·DNA) is active for subsequent dNTP binding and incorporation. The inclusion of step 3 in the proposed mechanism is consistent with the binary crystal structure in which the terminal base pair occupies the dNTP binding site (E·DNA*) and must be repositioned to allow nucleotide binding in a productive conformation (E·DNA).[8]

In previous stopped-flow FRET studies, a very rapid step occurring prior to the P_1 phase was attributed to a translocation of the DNA relative to Dpo4,[28] corresponding to a shift in equilibrium from the nonproductive state to the productive state. In a recent single-molecule FRET investigation, Dpo4 was observed to alternate between these two conformations in the binary complex, with the binding of an incoming dNTP stabilizing the post-translocated (E·DNA) productive state,[37] lending further support to the inclusion of step 3 in the proposed model (Figure 6C). This rapid conformational rearrangement was also proposed for the Y-family DNA polymerases from *Sulfolobus acidocaldarius* (Dbh)-based

stopped-flow fluorescence measurements with a DNA substrate containing a 2-aminopurine fluorescent base analogue.[38]

The observed rate of 0.02 s^{-1} in ^{32}P-based kinetic assays corresponds to the loss of only the catalytically competent E·DNA complex (k_{-3}) rather than much faster steps (k_{-1} and k_{-2}), as the assay relies on observation of a decreasing amount of nucleotide incorporation product following the increased incubation time with the trap DNA.[7] In our stopped-flow assays, the observed increase in fluorescence upon mixing Dpo4 with DNA (Figure 3A) would result from a shift in the equilibrium from the E^{apo} state to the E state [k_1 (Figure 6C)] followed by steps 2 and 3 that do not lead to a change in fluorescence. Similarly, the decrease in fluorescence upon mixing the Trp-containing or labeled Dpo4 mutant·DNA complex with unlabeled wt Dpo4 (Figure 3C,D) results from the shift in equilibrium back toward the E^{apo} state [k_{-1} (Figure 6C)] following a more rapid dissociation of the E·DNA* complex in step 2. Notably, without step 3 in the proposed model in Figure 6C (i.e., the model in Figure 6B), one would expect the rate measured in panels C and D of Figure 3 to be much slower as observed in the previously described ^{32}P-based kinetic trap assay, as k_{-3} (step 3, Figure 6C) would likely be lower at 20 °C than the value of 0.02 s^{-1} measured at 37 °C.[7]

Clearly, the binding of Dpo4 to DNA is a complex process, and while the FRET data described here provide new insight into an early conformational change in the binding pathway, further investigation is necessary to fully elucidate the binding mechanism. To this end, additional stopped-flow as well as single-molecule fluorescence studies to further probe the complex mechanism of binding of DNA to Dpo4 are currently underway.

The conformational change in the orientation of the LF domain upon DNA binding may be a phenomenon common to all Y-family DNA polymerases. As with Dpo4, crystal structures of human DNA polymerases κ (hPolκ) also show a change of up to 50 Å in the position of the LF domain relative to the polymerase core between the apo and DNA-bound states.[39,40] Furthermore, yeast DNA polymerase η (yPolη) also undergoes a structural change upon DNA binding, although it is much more modest, consisting of an 8° rotation of the LF domain.[25,41,42] Interestingly, the LF domain of hPolκ was

observed in two different conformations in the apo state, both of which are distinct from the conformation observed in the DNA-bound state.[39,40] While only one conformation of the LF domain has been observed for Dpo4 in the apo state, the crystal structure of Dpo4 in complex with the sliding clamp replication factor shows that the LF domain adopts a conformation different from that observed in the apo or DNA-bound form.[10] This suggests that a certain degree of conformational flexibility exists in the position of the LF domain even in the absence of a DNA substrate for these Y-family DNA polymerases, which is consistent with the inclusion of step 1 in the proposed model (Figure 6C). However, further structural and kinetic investigations are necessary to determine whether the kinetic mechanism proposed here will apply to other Y-family DNA polymerases.

In structural studies with both Dpo4[10] and the bacterial Y-family enzyme *Escherichia coli* DNA polymerase IV,[43] it was suggested each of the DNA polymerases primarily binds to a sliding clamp through its interactions with the LF domain in an inactive conformation that cannot bind to DNA, and thus, a conformational change would be required to allow for DNA binding by the Y-family DNA polymerase. To this end, it is possible that the conformational change in the LF domain prior to DNA binding (step 1, Figure 6C) may serve as a point of regulation during polymerase switching to prevent the low-fidelity Y-family DNA polymerases from accessing the replication fork prior to stalling of the replicative polymerases at DNA lesion sites.

Differences in DNA dissociation rates as measured by fluorescence versus ^{32}P-based kinetic assays have also been reported for A-family[44−46] and B-family[47,48] DNA polymerases as well, suggesting that these DNA polymerase families may utilize a multistep DNA binding mechanism similar to that of Dpo4. For example, crystal structures of the large fragment of *Thermus aquaticus* DNA polymerase I (Klentaq1) show that, in the E·DNA binary complex, the template base of the DNA substrate stacks with a conserved Tyr residue, and thus, a conformational rearrangement is required for dNTP binding.[49] Subsequently, stopped-flow FRET investigations with Klentaq1[36] and the Klenow fragment of *E. coli* DNA polymerase I[50] have revealed evidence of a pre-equilibrium step prior to nucleotide binding similar to step 3 in the proposed Dpo4 mechanism (Figure 6C). However, because other DNA polymerase families do not possess a domain analogous to the LF domain, it is unclear whether a transition analogous to step 1 in the proposed mechanism (Figure 6C) might be a general feature for DNA polymerases beyond those in the Y-family.

The interdomain FRET changes observed upon mixing a preformed Dpo4·DNA binary complex with dNTP (Figures 4 and 5) are consistent with the previously proposed nucleotide incorporation mechanism involving pre- and postcatalytic conformational change steps (steps 4−10, Figure 6C).[28] The biphasic traces observed with the Trp donor in the LF domain and the CPM acceptor in the Palm domain here (Figure 4) or in the Finger domain in a previous study[28] suggested that the LF domain moved away from the polymerase core before catalysis [P_1 (Figure 6C)] and returned toward it after catalysis [P_2 (Figure 6C)]. Similar results were obtained using mutant Y108W-S307C^{CPM} (Figure 5F), which also allowed us to monitor the change in distance between the Palm and LF domains. These observations are consistent with previous studies that showed that the LF domain also moves in a similar

fashion relative to the DNA substrate[28] and is further supported by computational predictions.[51]

Despite the similarity in the results obtained for the motion of LF residue Y274W relative to the Finger or Palm domain residues, the motion of the LF domain cannot be considered as a simple whole domain translational movement outward from the polymerase core and DNA substrate prior to catalysis, as revealed by mutant Y108W-K329C (Figure 5E). Mutant Y108W-K329C^{CPM} exhibited FRET changes in the opposite direction of those of all other FRET pairs between the LF and Palm domains. Inspection of the LF's crystal structure revealed that residues K329C and S307C are located on the loops on either side of α-helix M and that Y274W is located on α-helix L, near S307C (Figure 1).[9] A possible interpretation of the results of this study is that the LF domain rotates or bends about an axis perpendicular to helices M and L, where both residues S307C and Y274W are located on the one side of the axis and K329C is positioned on the other side of the axis. The possibility of a rotational axis is supported by molecular simulation, which suggests that the LF domain pivots around the DNA major groove by approximately 12°, as measured by the rotation of α helices L and M.[51] In previous FRET studies, similar rotational components were observed for the motion of the Finger and Palm domains relative to DNA during DNA lesion bypass.[28]

While most mutants exhibited two clear FRET phases, a clear P_2 phase was not apparent for mutants Y274W-S96C^{CPM} (black trace, Figure 4B) and Y108W-N200C^{CPM} (black trace, Figure 5D). It is possible that a change in distance between the FRET pairs in these mutants occurs during P_2 but that the amplitude of this change is too small to be detected given the inherent noise in the stopped-flow data. Conversely, the possibility that additional conformational change steps may be occurring during incorporation of the nucleotide by Dpo4 that complicate the data analysis for these particular FRET pairs cannot be ruled out. The observation of a second fluorescence phase for mutant Y108W-S307C^{CPM} even with the dideoxy-terminated primer (red trace, Figure 5F) may result from an additional conformational change step that occurs at a rate similar to the steps that give rise to P_2 for the other mutants but is independent of covalent nucleotide incorporation. If such a step also affects the motions of the FRET pairs in mutants Y274W-S96C^{CPM} and Y108W-N200C^{CPM}, it may obscure the P_2 phase for these mutants. However, the results of this study are not sufficient to determine whether this additional step or some other mechanistic phenomenon is responsible for the observed fluorescence changes in these three mutants.

It is clear from these FRET studies that the conformational dynamics of Dpo4 are complicated, and while the use of multiple FRET pairs allows us to provide some insight into the structural details of these conformational changes, further solution-state structure studies are necessary to gain a clear picture of how each domain moves throughout the entire reaction pathway. Recent chemical shift assignments of the backbone nitrogens, α and β carbons, and amide protons of the polymerase core[52] and the LF domain[53] of Dpo4 will likely facilitate future investigations of this nature at atomic resolution.

This work provides fresh insight into the importance of domain motions of Dpo4 to both DNA binding and catalysis and creates a global, complex dynamic picture of domain motions during the catalytic cycle. It would be very interesting to determine whether Dpo4 employs different conformational

motions while incorporating correct or incorrect dNTP into undamaged DNA or encountering and bypassing a variety of lesions. Future research to answer these questions will provide us the basis for understanding the mechanism of the reactions that Y-family DNA polymerases were evolved to catalyze.

■ ASSOCIATED CONTENT

Ⓢ Supporting Information

Figures showing the CD spectra of wt Dpo4 and several representative mutants and stopped-flow control experiments. This material is available free of charge via the Internet at http://pubs.acs.org.

■ AUTHOR INFORMATION

Corresponding Author

*Department of Chemistry and Biochemistry, The Ohio State University, 880 Biological Sciences Building, 484 West 12th Ave., Columbus, OH 43210. E-mail: suo.3@osu.edu. Telephone: (614) 688-3706. Fax: (614) 292-6773.

Notes

The authors declare no competing financial interest.

■ ACKNOWLEDGMENTS

■ ABBREVIATIONS

CPM, 7-(diethylamino)-3-(4′-maleimidylphenyl)-4-methylcoumarin; Dpo4, *S. solfataricus* DNA polymerase IV; FRET, Förster resonance energy transfer; LF, Little Finger; DNA^H, DNA substrate 21/30-mer containing a 3′-dideoxy-terminated 21-mer; DNA^{OH}, normal DNA substrate 21/30-mer; wt, wild-type; PDB, Protein Data Bank.

■ REFERENCES

(1) Yang, W., and Woodgate, R. (2007) What a difference a decade makes: Insights into translesion DNA synthesis. *Proc. Natl. Acad. Sci. U.S.A.* 104, 15591−15598.

(2) Matsuda, T., Bebenek, K., Masutani, C., Hanaoka, F., and Kunkel, T. A. (2000) Low fidelity DNA synthesis by human DNA polymerase-η. *Nature* 404, 1011−1013.

(3) Johnson, R. E., Washington, M. T., Haracska, L., Prakash, S., and Prakash, L. (2000) Eukaryotic polymerases ι and ζ act sequentially to bypass DNA lesions. *Nature* 406, 1015−1019.

(4) Zhang, Y., Yuan, F., Xin, H., Wu, X., Rajpal, D. K., Yang, D., and Wang, Z. (2000) Human DNA polymerase κ synthesizes DNA with extraordinarily low fidelity. *Nucleic Acids Res.* 28, 4147−4156.

(5) Wang, Z. (2001) Translesion synthesis by the UmuC family of DNA polymerases. *Mutat. Res.* 486, 59−70.

(6) Fiala, K. A., Abdel-Gawad, W., and Suo, Z. (2004) Pre-Steady-State Kinetic Studies of the Fidelity and Mechanism of Polymerization Catalyzed by Truncated Human DNA Polymerase λ. *Biochemistry* 43, 6751−6762.

(7) Fiala, K. A., and Suo, Z. (2004) Mechanism of DNA Polymerization Catalyzed by *Sulfolobus solfataricus* P2 DNA Polymerase IV. *Biochemistry* 43, 2116−2125.

(8) Wong, J. H., Fiala, K. A., Suo, Z., and Ling, H. (2008) Snapshots of a Y-family DNA polymerase in replication: Substrate-induced conformational transitions and implications for fidelity of Dpo4. *J. Mol. Biol.* 379, 317−330.

(9) Ling, H., Boudsocq, F., Woodgate, R., and Yang, W. (2001) Crystal structure of a Y-family DNA polymerase in action: A mechanism for error-prone and lesion-bypass replication. *Cell* 107, 91−102.

(10) Xing, G., Kirouac, K., Shin, Y. J., Bell, S. D., and Ling, H. (2009) Structural insight into recruitment of translesion DNA polymerase Dpo4 to sliding clamp PCNA. *Mol. Microbiol.* 71, 678−691.

(11) Rechkoblit, O., Malinina, L., Cheng, Y., Kuryavyi, V., Broyde, S., Geacintov, N. E., and Patel, D. J. (2006) Stepwise translocation of Dpo4 polymerase during error-free bypass of an oxoG lesion. *PLoS Biol.* 4, e11.

(12) Eoff, R. L., Irimia, A., Angel, K. C., Egli, M., and Guengerich, F. P. (2007) Hydrogen bonding of 7,8-dihydro-8-oxodeoxyguanosine with a charged residue in the little finger domain determines miscoding events in *Sulfolobus solfataricus* DNA polymerase Dpo4. *J. Biol. Chem.* 282, 19831−19843.

(13) Trincao, J., Johnson, R. E., Wolfle, W. T., Escalante, C. R., Prakash, S., Prakash, L., and Aggarwal, A. K. (2004) Dpo4 is hindered in extending a G.T mismatch by a reverse wobble. *Nat. Struct. Mol. Biol.* 11, 457−462.

(14) Fiala, K. A., and Suo, Z. (2004) Pre-Steady-State Kinetic Studies of the Fidelity of *Sulfolobus solfataricus* P2 DNA Polymerase IV. *Biochemistry* 43, 2106−2115.

(15) Sherrer, S. M., Brown, J. A., Pack, L. R., Jasti, V. P., Fowler, J. D., Basu, A. K., and Suo, Z. (2009) Mechanistic Studies of the Bypass of a Bulky Single-base Lesion Catalyzed by a Y-family DNA Polymerase. *J. Biol. Chem.* 284, 6379−6388.

(16) Boudsocq, F., Iwai, S., Hanaoka, F., and Woodgate, R. (2001) *Sulfolobus solfataricus* P2 DNA polymerase IV (Dpo4): An archaeal DinB-like DNA polymerase with lesion-bypass properties akin to eukaryotic polη. *Nucleic Acids Res.* 29, 4607−4616.

(17) Fiala, K. A., Hypes, C. D., and Suo, Z. (2007) Mechanism of abasic lesion bypass catalyzed by a Y-family DNA polymerase. *J. Biol. Chem.* 282, 8188−8198.

(18) Frauenfelder, H., Sligar, S. G., and Wolynes, P. G. (1991) The energy landscapes and motions of proteins. *Science* 254, 1598−1603.

(19) Hammes-Schiffer, S., and Benkovic, S. J. (2006) Relating protein motion to catalysis. *Annu. Rev. Biochem.* 75, 519−541.

(20) Herbst, K. J., Ni, Q., and Zhang, J. (2009) Dynamic visualization of signal transduction in living cells: From second messengers to kinases. *IUBMB Life* 61, 902−908.

(21) Hammes, G. G. (2002) Multiple conformational changes in enzyme catalysis. *Biochemistry* 41, 8221−8228.

(22) Panke, S., and Wubbolts, M. G. (2002) Enzyme technology and bioprocess engineering. *Curr. Opin. Biotechnol.* 13, 111−116.

(23) Silvian, L. F., Toth, E. A., Pham, P., Goodman, M. F., and Ellenberger, T. (2001) Crystal structure of a DinB family error-prone DNA polymerase from *Sulfolobus solfataricus*. *Nat. Struct. Biol.* 8, 984−989.

(24) Boudsocq, F., Kokoska, R. J., Plosky, B. S., Vaisman, A., Ling, H., Kunkel, T. A., Yang, W., and Woodgate, R. (2004) Investigating the role of the little finger domain of Y-family DNA polymerases in low fidelity synthesis and translesion replication. *J. Biol. Chem.* 279, 32932−32940.

(25) Trincao, J., Johnson, R. E., Escalante, C. R., Prakash, S., Prakash, L., and Aggarwal, A. K. (2001) Structure of the catalytic core of *S. cerevisiae* DNA polymerase η: Implications for translesion DNA synthesis. *Mol. Cell* 8, 417−426.

(26) Doublie, S., Sawaya, M. R., and Ellenberger, T. (1999) An open and closed case for all polymerases. *Structure* 7, R31−R35.

(27) Beckman, J. W., Wang, Q., and Guengerich, F. P. (2008) Kinetic analysis of correct nucleotide insertion by a Y-family DNA polymerase reveals conformational changes both prior to and following phosphodiester bond formation as detected by tryptophan fluorescence. *J. Biol. Chem.* 283, 36711−36723.

(28) Xu, C., Maxwell, B. A., Brown, J. A., Zhang, L., and Suo, Z. (2009) Global conformational dynamics of a Y-family DNA polymerase during catalysis. *PLoS Biol. 7*, e1000225.

(29) Eoff, R. L., Sanchez-Ponce, R., and Guengerich, F. P. (2009) Conformational changes during nucleotide selection by *Sulfolobus solfataricus* DNA polymerase Dpo4. *J. Biol. Chem. 284*, 21090−21099.

(30) Maxwell, B. A., Xu, C., and Suo, Z. (2012) DNA Lesion Alters Global Conformational Dynamics of Y-family DNA Polymerase during Catalysis. *J. Biol. Chem. 287*, 13040−13047.

(31) Zhang, H., and Guengerich, F. P. (2010) Effect of N2-guanyl modifications on early steps in catalysis of polymerization by *Sulfolobus solfataricus* P2 DNA polymerase Dpo4 T239W. *J. Mol. Biol. 395*, 1007−1018.

(32) Sherrer, S. M., Maxwell, B. A., Pack, L. R., Fiala, K. A., Fowler, J. D., Zhang, J., and Suo, Z. (2012) Identification of an unfolding intermediate for a DNA lesion bypass polymerase. *Chem. Res. Toxicol. 25*, 1531−1540.

(33) Johnson, K. A., Simpson, Z. B., and Blom, T. (2009) Global Kinetic Explorer: A new computer program for dynamic simulation and fitting of kinetic data. *Anal. Biochem. 387*, 20−29.

(34) Chakraborty, S., Ittah, V., Bai, P., Luo, L., Haas, E., and Peng, Z. (2001) Structure and dynamics of the α-lactalbumin molten globule: Fluorescence studies using proteins containing a single tryptophan residue. *Biochemistry 40*, 7228−7238.

(35) Lakowicz, J. R. (1999) *Principles of fluorescence spectroscopy*, 2nd ed., Kluwer Academic/Plenum, New York.

(36) Rothwell, P. J., and Waksman, G. (2007) A pre-equilibrium before nucleotide binding limits fingers subdomain closure by Klentaq1. *J. Biol. Chem. 282*, 28884−28892.

(37) Brenlla, A., Markiewicz, R. P., Rueda, D., and Romano, L. J. (2014) Nucleotide selection by the Y-family DNA polymerase Dpo4 involves template translocation and misalignment. *Nucleic Acids Res. 42*, 2555−2563.

(38) DeLucia, A. M., Grindley, N. D., and Joyce, C. M. (2007) Conformational changes during normal and error-prone incorporation of nucleotides by a Y-family DNA polymerase detected by 2-aminopurine fluorescence. *Biochemistry 46*, 10790−10803.

(39) Uljon, S. N., Johnson, R. E., Edwards, T. A., Prakash, S., Prakash, L., and Aggarwal, A. K. (2004) Crystal structure of the catalytic core of human DNA polymerase κ. *Structure 12*, 1395−1404.

(40) Lone, S., Townson, S. A., Uljon, S. N., Johnson, R. E., Brahma, A., Nair, D. T., Prakash, S., Prakash, L., and Aggarwal, A. K. (2007) Human DNA polymerase κ encircles DNA: Implications for mismatch extension and lesion bypass. *Mol. Cell 25*, 601−614.

(41) Alt, A., Lammens, K., Chiocchini, C., Lammens, A., Pieck, J. C., Kuch, D., Hopfner, K. P., and Carell, T. (2007) Bypass of DNA lesions generated during anticancer treatment with cisplatin by DNA polymerase η. *Science 318*, 967−970.

(42) Silverstein, T. D., Johnson, R. E., Jain, R., Prakash, L., Prakash, S., and Aggarwal, A. K. (2010) Structural basis for the suppression of skin cancers by DNA polymerase η. *Nature 465*, 1039−1043.

(43) Bunting, K. A., Roe, S. M., and Pearl, L. H. (2003) Structural basis for recruitment of translesion DNA polymerase Pol IV/DinB to the β-clamp. *EMBO J. 22*, 5883−5892.

(44) Berezhna, S. Y., Gill, J. P., Lamichhane, R., and Millar, D. P. (2012) Single-molecule Forster resonance energy transfer reveals an innate fidelity checkpoint in DNA polymerase I. *J. Am. Chem. Soc. 134*, 11261−11268.

(45) Christian, T. D., Romano, L. J., and Rueda, D. (2009) Single-molecule measurements of synthesis by DNA polymerase with base-pair resolution. *Proc. Natl. Acad. Sci. U.S.A. 106*, 21109−21114.

(46) Kuchta, R. D., Mizrahi, V., Benkovic, P. A., Johnson, K. A., and Benkovic, S. J. (1987) Kinetic mechanism of DNA polymerase I (Klenow). *Biochemistry 26*, 8410−8417.

(47) Brown, J. A., and Suo, Z. (2009) Elucidating the kinetic mechanism of DNA polymerization catalyzed by *Sulfolobus solfataricus* P2 DNA polymerase B1. *Biochemistry 48*, 7502−7511.

(48) Maxwell, B. A., and Suo, Z. (2013) Single-molecule Investigation of Substrate Binding Kinetics and Protein Conforma-tional Dynamics of a B-family Replicative DNA Polymerase. *J. Biol. Chem. 288*, 11590−11600.

(49) Li, Y., Korolev, S., and Waksman, G. (1998) Crystal structures of open and closed forms of binary and ternary complexes of the large fragment of *Thermus aquaticus* DNA polymerase I: Structural basis for nucleotide incorporation. *EMBO J. 17*, 7514−7525.

(50) Joyce, C. M., Potapova, O., Delucia, A. M., Huang, X., Basu, V. P., and Grindley, N. D. (2008) Fingers-closing and other rapid conformational changes in DNA polymerase I (Klenow fragment) and their role in nucleotide selectivity. *Biochemistry 47*, 6103−6116.

(51) Wang, Y., Arora, K., and Schlick, T. (2006) Subtle but variable conformational rearrangements in the replication cycle of *Sulfolobus solfataricus* P2 DNA polymerase IV (Dpo4) may accommodate lesion bypass. *Protein Sci. 15*, 135−151.

(52) Ma, D., Fowler, J. D., Yuan, C., and Suo, Z. (2010) Backbone assignment of the catalytic core of a Y-family DNA polymerase. *Biomol. NMR Assignments 4*, 207−209.

(53) Ma, D., Fowler, J. D., and Suo, Z. (2011) Backbone assignment of the little finger domain of a Y-family DNA polymerase. *Biomol. NMR Assignments 5*, 195−198.